Functionalizing Carbon Nanotubes by Plasma Modification for the Preparation of Covalent-Integrated Epoxy Composites

Chun-Hao Tseng,[†] Cheng-Chien Wang,[‡] and Chuh-Yung Chen*,[†]

Department of Chemical Engineering, National Cheng Kung University, 70101, Tainan, Taiwan, and Department of Chemical Engineering and Material Engineering, Southern Taiwan University of Technology, 710, Tainan, Taiwan

Received September 22, 2006. Revised Manuscript Received November 5, 2006

A novel method for preparing a fully integrated nanotube composite material through the use of functionalized multi-walled carbon nanotubes (MWNTs) is presented in this study. The functionalization of MWNTs was performed via plasma treatment; subsequently, maleic anhydride (MA) was grafted onto the MWNTs (CNTs-MA). Nanotube-reinforced epoxy polymer composites were prepared by first mixing the CNTs-MA and a diamine curing agent, followed by a further reaction with the epoxy matrix. In this hybrid nanocomposite system, the CNTs-MA were covalently integrated into the epoxy matrix and became part of the cross-linked structure rather than just a separate component. Fourier transform infrared (FT-IR) and high resolution X-ray photoelectron (XPS) spectroscopes were used to characterize the functional groups on the surface of the MWNTs after the plasma modification. In addition, observations of scanning electronic microscopy (SEM) and transmission electron microscopy (TEM) images showed that the functionalized nanotubes, CNTs-MA, had a better dispersion than the unfunctionalized nanotubes, u-CNTs, on either the composite fracture surfaces or inside the epoxy matrix. Moreover, CNTs-MA/epoxy nanocomposites presented obvious improvements in mechanical properties and conductivity (from 10^{-12} to 10^{-4} S/m) with only a small quantity (0.1−1.0 wt %) of the CNTs-MA addition.

Introduction

Carbon nanotubes (CNTs) have attracted considerable attention because of their extraordinary properties (high strength and flexibility, high thermal and electrical conductivity, and low density), leading them to be used for the preparation of nanotube-reinforced composites.[1,2] Among polymer composites, high strength epoxy systems are very important materials for aircraft, space shuttles, electronic products, as well as numerous other industrial applications. Nanotube-reinforced epoxy systems hold the promise of delivering superior composite materials with high strength, light weight, and multi-functional features. However, the field that seeks to incorporate CNTs as polymer composite reinforcements has been beset by a number of crucial problems. Because of strong intrinsic van der Waals forces, CNTs tend to hold together as ropes and bundles having very low solubility in most solvents, which leads to poor dispersion when mixed into the polymer matrix. Moreover, the atomically smooth surface of nanotubes, and lack of interfacial bonding, limits load transfer from the polymer matrix to the nanotubes. Therefore, the ability to disperse the CNTs homogeneously inside the polymer matrix, as well as the ability to produce a strong interfacial interaction between CNTs and polymers, will be key issues in maximizing the advantage of CNTs reinforcement.

A great deal of research has been carried out to improve the dispersion of CNTs, as well as to functionalize CNTs to produce strong chemical bonding to the polymer matrix. This research has included investigation of methods such as optimum physical blending[3,4] (ultrasonication and high shear mixing), aid of surfactants,[5] in situ polymerization,[6−8] and chemical functionalization.[9−12] For Example, Chou et al.[3] dispersed MWNTs into epoxy polymer by severe shear mixing and showed an increase of thermal conductivity of 60% with 5 wt % addition of MWNTs. Gong et al.[5] used a non-ionic surfactant, polyoxyethylene 8-lauryl, as a processing aid for an epoxy/CNTs composite. With 1 wt % CNTs in the epoxy/CNTs composites, the elastic modulus increased by over 30% and the glass transition temperature by 25 °C. Carlos et al.[6] synthesized PMMA/MWNT composites by in

---

* To whom correspondence should be addressed. E-mail: ccy7@ccmail.ncku.edu.tw. Tel.: +886-6-2360468. Fax: +886-6-2344496.
[†] National Cheng Kung University.
[‡] Southern Taiwan University of Technology.

(1) Calvert, P. *Nature* **1999**, *399*, 210−211.
(2) Wagner, H. D.; Lourie, O.; Feldman, Y.; Tenne, R. *Appl. Phys. Lett.* **1998**, *72*, 188−190.
(3) Thostenson, E. T.; Chou, T. W. *Carbon* **2006**, *44*, 3022−3029.
(4) Vaccarini, L.; Désarmot, G.; Almairac, R.; Tahir, S.; Goze, C.; Bernier, P. *AIP Conf. Proc.* **2000**, *544*, 521−525.
(5) Gong, X.; Liu, J.; Baskaran, S.; Roger, D. V.; Young, J. S. *Chem. Mater.* **2000**, *12*, 1049−1052.
(6) Carlos, V. S.; Ana, L. M. H.; Frank, T. F.; Rodney, R.; Victor, M. C. *Chem. Mater.* **2003**, *15*, 4470−4475.
(7) Tang, B. Z.; Xu, H. *Macromolecules* **1999**, *32*, 2569−2576.
(8) Cochet, M.; Maser, W. K.; Benitor, A.; Callejas, A.; Martinez, M. T.; Benoit, J. M.; Schreiber, J.; Chauvet, O. *Chem. Commum.* **2001**, 1450−1451.
(9) Zhu, J.; Kim, J.; Peng, H.; Margrave, J. L.; Khabashesku, V. N.; Barrera, E. V. *Nano Lett.* **2003**, *3*, 1107−1113.
(10) Andrew, J. L.; Rinzler, G.; Dai, H.; Hafner, J. H.; Bradley, R. K.; Boul, P. J.; Lu, A.; Iverson, T.; Shelimov, K.; Huffman, C. B.; Rodriguez-Macias, F.; Shon, Y. S.; Lee, T. R.; Colbert, D. T.; Smalley, R. E. *Science* **1998**, *280*, 1253−1256.
(11) Kim, B.; Sigmund, W. M. *Langmuir* **2004**, *20*, 8239−8242.
(12) Li, Y. H.; Wang, S.; Luan, Z.; Ding, J.; Xu, C.; Wu, D. *Carbon* **2003**, *41*, 1057−1062.

10.1021/cm062277p CCC: $37.00

Scheme 1. Overall Procedure for Preparation of CNTs-MA/Epoxy Nanocomposites

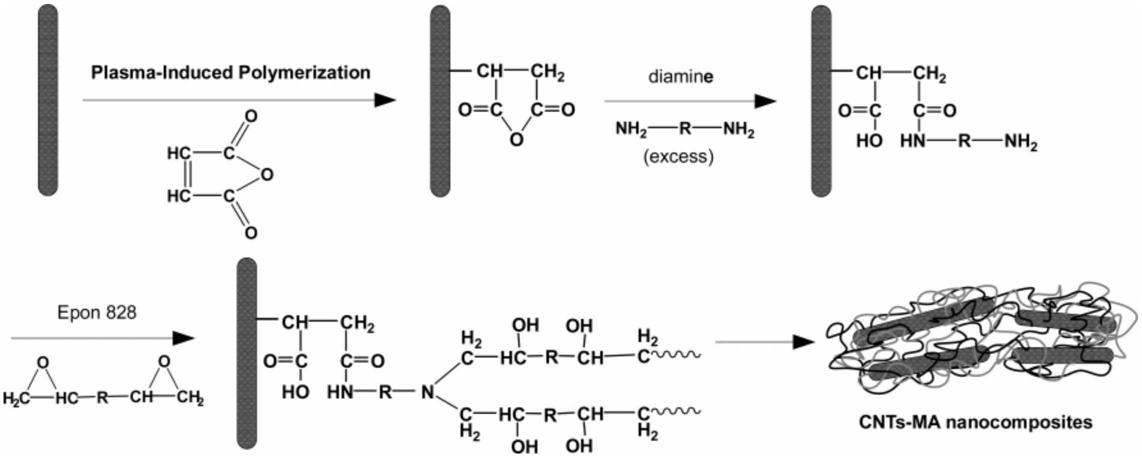

situ polymerization. Their results revealed an increase in the storage modulus from 1561 to 2539 MPa at a temperature of 40 °C with 1 wt % addition of CNTs. All of the methods described previously show an improvement in the dispersion of CNTs inside the polymer matrix to achieve well-dispersed CNT/composites. However, the previous experimental data have shown weak interfacial bonding between pristine nanotubes and polymer matrix and therefore limited load-transfer ability. The high performance CNT reinforcement composites can only be obtained by adding large quantities of CNTs.

An external tensile load can be effectively transferred from the matrix to the nanotubes only when the CNTs are functionalized with strong chemical bonding to the matrix.[9−12] Numerous methods for chemical functionalization of carbon nanotubes have already been reported. Zhu et al.[9] functionalized SWNTs by using an acid treatment and subsequent fluorination. The results showed an enhancement in mechanical properties: a 30% increase in modulus and 18% increase in tensile strength. However, the processes in the functionalization of CNTs by acid treatment are complex and difficult to control. Moreover, several research reports[13−15] have shown that strong acid modification such as HNO_3 and H_2SO_4 treatments lead the CNTs to be easily damaged in the structure of the tube walls and can even cut the length of the CNTs, which limits further applications as reinforcement composites.

Among these techniques of modifying CNTs, the plasma-treatment method is important since it has the advantage of being nonpolluting, which is not negligible for an industrial fabrication. It has the possibility of scaling up to produce large quantities necessary for commercial use. Several methods of plasma modification of the CNTs have been reported.[13−15] For example, Dai et al.[16] functionalized CNTs with an amino-dextran chain via acetaldehyde plasma treatment. Meyyappan et al.[17] modified the surface of single-walled carbon nanotubes by using CF_4 microwave plasma. Charlier et al.[18] used rf-plasma treatment to graft oxygen-, nitrogen-, and fluorine-containing groups on the surface of the MWNTs. However, to date, using the plasma-modified carbon nanotubes as nanotube-reinforced nanocomposites has not been reported yet. Herein, we seek to develop a fully integrated nanotube−epoxy polymer composite system via direct treatment by plasma and subsequent functionalization of the MWNTs by grafting maleic anhydride onto the tube walls. The MWNTs grafted with maleic anhydride (CNTs-MA) can readily react with diamine, which acts as a curing agent for the epoxy matrix. The functionalized CNTs with amino groups attached enable the nanotubes to become chemically bonded to the matrix and become an integral part of the composite. The advantage of the in situ technique is not only that the process of functionalization can be achieved in a simple step but also that the MWNTs are preserved in their original length after the plasma modification, which allows more extensive applications as reinforcement materials.

Experimental Procedures

Materials. The MWNTs used in this work were purchased from the Industrial Technology Research Institute in Taiwan and were synthesized by ethylene CVD using Al_2O_3 supported Fe_2O_3 catalysts.[19] The purity is higher than 95%. Before the modification of plasma treatment, the MWNTs were purified by sonicating in 25 wt % hydrochloric acid for 40 min to remove the catalysts and then diluting with deionized water by filtration through a 0.1 μm membrane filter (Gelman). After that, the obtained MWNTs were heated in air for 1.5 h at 600 °C to oxidize the amorphous carbon. Finally, purified MWNTs were obtained by annealing in N_2 at 950 °C to remove the oxygen-based functional groups generated from the thermal treatment. The diameters of the purified MWNTs were in the range of 10 to ~90 nm. Maleic anhydride (MA) (Aldrich Co.), diglycidyl ether of bisphenol A (Shell EPON 828, MW = 377), and curing agent *N*,*N*′-bis(2-aminopropyl) polypropylene glycol (Aldrich Co., MW = 400) were used as received.

---

(13) Hu, H.; Yu, A.; Kim, E.; Zhao, B.; Itkis, M. E.; Bekyarova, E.; Haddon, R. C. *J. Phys. Chem. B* **2005**, *109*, 11520−11524.

(14) Grossiord, N.; Loos, J.; Regev, O.; Koning, C. E. *Chem. Mater.* **2006**, *18*, 1089−1099.

(15) Park, S. J.; Cho, M. S.; Lim, S. T.; Choi, H. J.; Jhon, M. S. *Macromol. Rapid Commun.* **2003**, *24*, 1070−1073.

(16) Chen, Q.; Dai, L.; Gao, M.; Huang, S.; Mau, A. *J. Phys. Chem. B* **2001**, *105*, 618−622.

(17) Khare, B. N.; Wilhite, P.; Meyyappan, M. *Nanotechnology* **2004**, *15*, 1650−1654.

(18) Felten, A.; Bittencourt, C.; Pireaux, J. J.; Van Lier, G.; Charlier, J. C. *J. Appl. Phys.* **2005**, *98*, 074308−9.

(19) Qian, W. Z.; Wei, F.; Wang, Z. W.; Liu, T. *AICHE J.* **2003**, *49*, 619−625.

(20) Tseng, C. H.; Wang, C. C.; Chen, C. Y. *J. Phys. Chem. B* **2006**, *110*, 4020−4029.

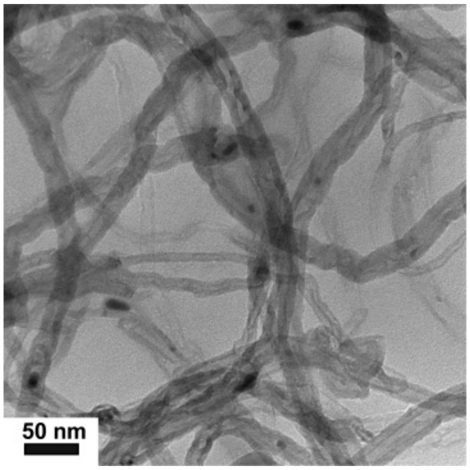

Figure 1. TEM image of the funtionalized nanotubes, CNTs-MA.

Preparation of MWNTs Grafted Maleic Anhydride (CNTs-MA) by Plasma Treatment. The plasma treatment was carried out in a parallel plane electrode reactor, and the volume of the stainless steel vacuum chamber was about 6×10^3 cm^3. The electrodes were made of circular Cu plates (diameter = 5 cm) that were separated at a distance of 3 cm. The MWNTs were spread regularly on the chamber and exposed to plasma treatment for 5 min. Prior to starting up the plasma reaction, the pressure was reduced to 10^{-6} Torr in the reactor. Then, pure Ar gas was introduced into the reactor via a leak valve at a flow rate of 20 mL/min, and the vacuum pressure of the plasma reactor was controlled precisely at 0.1 Torr by using the throttle valve. The electrical power of the plasma was supplied by an RF-power generator operating at 50 W and at 13.56 MHz. Details about the plasma modification follow the procedure established in our previous studies.[20−22] After the plasma treatment, a large number of radicals were generated on the surface of the MWNTs, and the maleic anhydride (MA) with a concentration of 0.1 M dissolved in toluene was injected into the reactor to graft onto the MWNTs at 50 °C for 3 h. After the grafting polymerization, the MWNTs grafted maleic anhydride, CNTs-MA, was washed by toluene 3 times and subsequently separated by centrifuging. The sediments were dried in a vacuum oven at 70 °C overnight to remove the solvent. The resulting products obtained were the functionalized MWNTs, CNTs-MA.

Preparation of the CNTs-MA/Epoxy Nanocomposites. The pristine epoxy resin was prepared by mixing EPON 828 with a diamine curing agent at 70 °C for 30 min, outgassing the mixture in a vacuum oven for 2 h, and curing by a thermal schedule (80 °C for 2 h, 120 °C for 2 h, and 140 °C for 4 h). For the preparation of the CNTs-MA/epoxy nanocomposites, first CNTs-MA were added into the diamine curing agent, and the mixture was shear mixed for 2 h and sonicated for another 15 min. Subsequently, Epon 828 resin was added and further shear mixed with the CNTs-MA/diamine mixture at 80 °C for 30 min. Finally, the resulting mixture was outgassed in a vacuum oven for 2 h and then cast into an aluminum mold. The curing cycle of CNTs-MA/epoxy nanocomposites is the same as that of the pristine epoxy. Scheme 1 illustrates the procedure of functionalization of the MWNTs and subsequent preparation of the CNTs-MA/epoxy nanocomposites.

Table 1. Atomic Concentration and Grafting Percentage of MA Determined from XPS Experiment Data

sample	atomic concentration (%) C 1s	atomic concentration (%) O 1s	MA grafting percentage (wt %)
u-CNTs	97.8	2.2	
CNTs-MA	95.4	4.6	6.4

Identification. Fourier transform infrared (FT−-IR) spectra were recorded with a Bio-Rad FTS-40A FT−-IR analyzer, which operated from 700 to 4000 cm^{-1} at room temperature. Spectra were obtained using a resolution of 4 cm^{-1} and were averaged over 16 scans. Before the IR measurement, MWNTs were ground thoroughly with potassium bromide (KBr) at approximately 3%, and the resulting powder was pressed into a transparent pellet. Hitachi S4200 field emission scanning electron microscopy (SEM) was used to observe the fractured surface of CNTs/epoxy nanocomposites with different CNT contents. Transmission electron microscope samples of the cross-section images were cut into slices of 60 nm thickness using a Leica UCT Microtome with a diamond knife. Samples were collected on the hexagonal 300 mesh copper grids. For TEM measurements of the funtionalized nanotubes, CNTs-MA were suspended in toluene solution and were drop cast onto a carbon-coated copper grid followed by solvent evaporation in air at room temperature. All of the TEM images were obtained using Hitachi HF-2000 field emission transmission electron microscopy (TEM) at an acceleration voltage of 200 kV. Tensile testing on samples was performed using an Instron-4464 Universal Tester at a strain rate of 5 mm/min with a dog-bone shape. To ensure data accuracy and repeatability, the results for five samples from different batches were averaged. X-ray photoemission spectrometry (XPS) was performed using an ESCA PHI 1600 machine equipped with a base pressure of 5×10^{-10} Torr. The monochromated Mg Kα X-radiation was used as the excitation source, and the instrument resolution was ~0.7 eV. XPS samples were prepared by placing the MWNTs on carbon conductive tape on the sample holder. The Au$4f_{7/2}$ peak (84.0 eV) was used for calibration. Thermogravimetric analyses (TGA) were performed using a Perkin-Elmer TAC 7/ DX analyzer. Samples were heated from room temperature to 800 °C at a heating rate of 20 °C/min under nitrogen purge. Thermal analysis of the CNTs/epoxy nanocomposites was carried out in a Dupont DSC 2910 differential scanning calorimeter with a heating rate of 20 °C/min and a temperature range of −40 to 100 °C. Impedance analysis was recorded by using Autolab PGSTAT 30 equipment (Eco Chemie B.V.) with Frequency Response Analysis (FRA) system software under an oscillation potential of 10 mV from 100 kHz at room temperature. The conductivity (σ) was calculated from the complex impedance (Z^*) according to $\sigma(\nu) = [1/Z^*(\nu)]t/A$, where t is the sample thickness and A is the cross-section area. The results of the electrical conductivity were averaged by five different samples.

Results and Discussion

Preparation of the CNTs-MA by Plasma Modification. Figure 1 is the TEM image of the functionalized MWNTs, CNTs-MA, after plasma-induced grafting polymerization. The image shows that the CNTs-MA, instead of showing crowded bundles, have a less tangled organization, which demonstrates that the grafted MA molecule efficiently promotes the dispersal of the MWNTs. Moreover, the CNTs-MA are still kept in their original length after plasma modification, which is different from the results obtained by chemical acid modification such as HNO_3 and H_2SO_4 treatments.[9−12]

---

(21) Tseng, C. H.; Wang, C. C.; Chen, C. Y. *J. Nanosci. Nanotechnol.* **2006**, *6*, 3897−3903.
(22) Tseng, C. H.; Wang, C. C.; Chen, C. Y. *Nanotechnology* **2006**, *17*, 5602−5612.

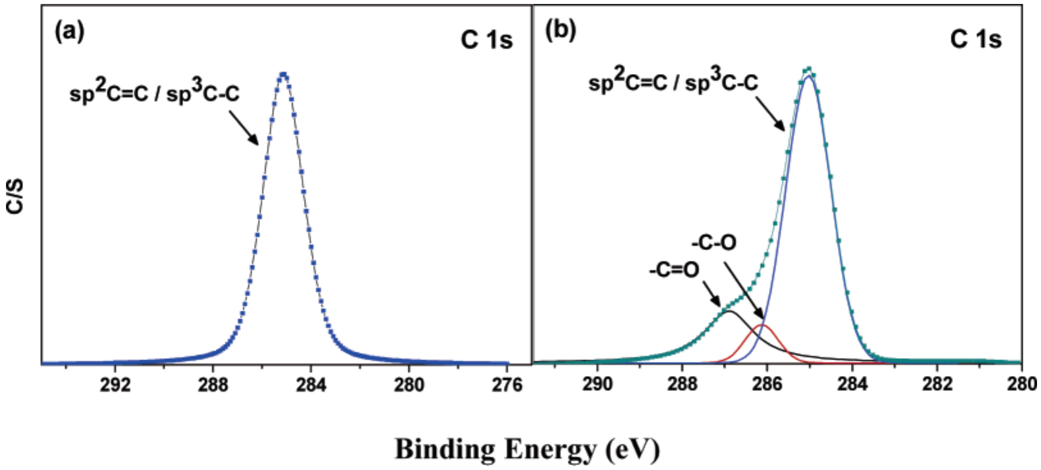

Figure 2. XPS core level spectra of C 1s of (a) u-CNTs and (b) CNTs-MA.

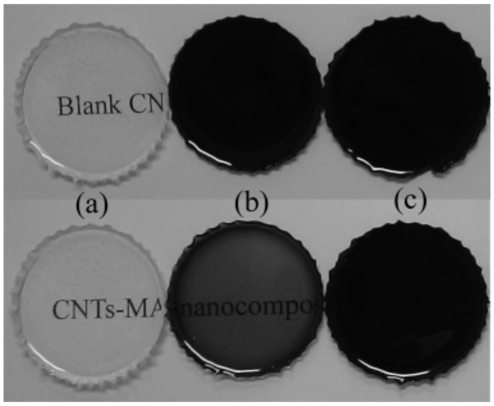

Figure 3. Photographs of CNTs/epoxy nanocomposites with various quantities of CNT content: (a) 0 wt %, (b) 0.1 wt %, and (c) 0.3 wt %. The upper row is the u-CNTs/epoxy nanocomposite, and the lower row is the CNTs-MA/epoxy nanocomposite.

In addition, XPS was utilized to individually elucidate the compositions of the u-CNTs and CNTs-MA. In each case, an initial broad scan was performed (1100−0 eV) to establish the gross elemental composition of the surface of the sample. Both the u-CNTs and the CNTs-MA show distinct carbon (C 1s, C KLL) and oxygen (O 1s, O KLL) peaks, thus presenting the major constituents of the sample surface. However, after the grafting of the MA unit, CNTs-MA have a slight increase in the O 1s peak as compared with the u-CNTs. The atomic concentrations obtained by XPS analysis reveal that the concentration of O 1s increased from 2.2 to 4.6 after the grafting of the MA unit. In addition, the MA grafting percentage was 6.4 wt %, which is estimated by the increasing amount of the O component. The experimental data are shown in Table 1.

Furthermore, detailed analysis of the XPS spectra provides clear evidence that the MWNTs have been chemically modified. As seen in Figure 2a, the carbon C 1s peak, observed at 284.3−285.5 eV, is interpreted as the combination of the sp^2 C═C and sp^3 C−C structures of the u-CNTs. After the plasma modification, CNTs-MA, the shoulder of the main peak is composed of two peaks, located at 286.2 and 287.1 eV, which originated from the −C−O and −C═O structures, respectively,[23−25] as depicted in Figure 2b. This graph provides evidence that the MWNTs have been functionalized by MA.

Preparation of the CNTs-MA/Epoxy Nanocomposites. In the composite fabrication process, the functionalized MWNTs, CNTs-MA, first reacted with the diamine and further chemically bonded with the epoxy via an amidation reaction. The amino groups attached to CNTs-MA can function as curing agents, which leads to the formation of a highly cross-linked structure by covalent bonds between the CNTs and the epoxy matrix. Figure 3 presents the photographs of the CNT/epoxy nanocomposites with various quantities of CNT content. Both the u-CNT/epoxy and the CNTs-MA/epoxy nanocomposites become more black and opaque with the increase of CNT loading. However, the CNTs-MA/epoxy nanocomposite with 0.1 wt % is translucent, as compared with the totally opaque u-CNT/epoxy nanocomposite. The result reveals that the functionalized CNTs-MA dispersed on the nanoscale and is more compatible with the epoxy matrix, leading to optical transparence at low CNTs-MA contents. In contrast, all the u-CNTs/epoxy nanocomposites are opaque, due to weak chemical bonding between the u-CNTs and the epoxy matrix, as well as the fact that they are easily aggregated inside the epoxy matrix. Moreover, as the content of the u-CNTs increases to 1.0 wt %, the composite has an obviously rough morphology because of large aggregations of the u-CNTs formed inside the epoxy matrix.

The SEM images of the composite fracture surfaces show the dispersion of the CNTs in the epoxy matrix. The fracture surfaces of the epoxy composites loaded with the unfunctionalized CNTs, u-CNTs, show nonuniform dispersion and the tendency for the nanotubes to entangle as agglomerates. The phenomenon of agglomeration becomes more pronounced as the loading of the u-CNTs increases (Figure 4a−e). Besides, most of the u-CNTs show sliding and pulling out at the surface, suggesting a limitation of load transfer. By comparison, the CNT-MA system shows good homoge-

---

(23) Okpalugo, T. I. T.; Papakonstantinou, P.; Murphy, H.; McLaughlin, J.; Brown, N. M. D. *Carbon* **2005**, *43*, 153−161.

(24) Urszula, D. W.; Viera, S.; Ralf, G.; Sung, H. J.; Byung, H. K.; Hyun, J. L.; Lothar, L.; Yung, W. P.; Savas, B.; David, T.; Siegmar, R. *J. Am. Chem. Soc.* **2005**, *127*, 5125−5131.

(25) Lee, W. H.; Kim, S. J.; Lee, W. J.; Lee, J. G.; Haddon, R. C.; Reucroft, P. J. *Appl. Surf. Sci.* **2001**, *181*, 121−127.

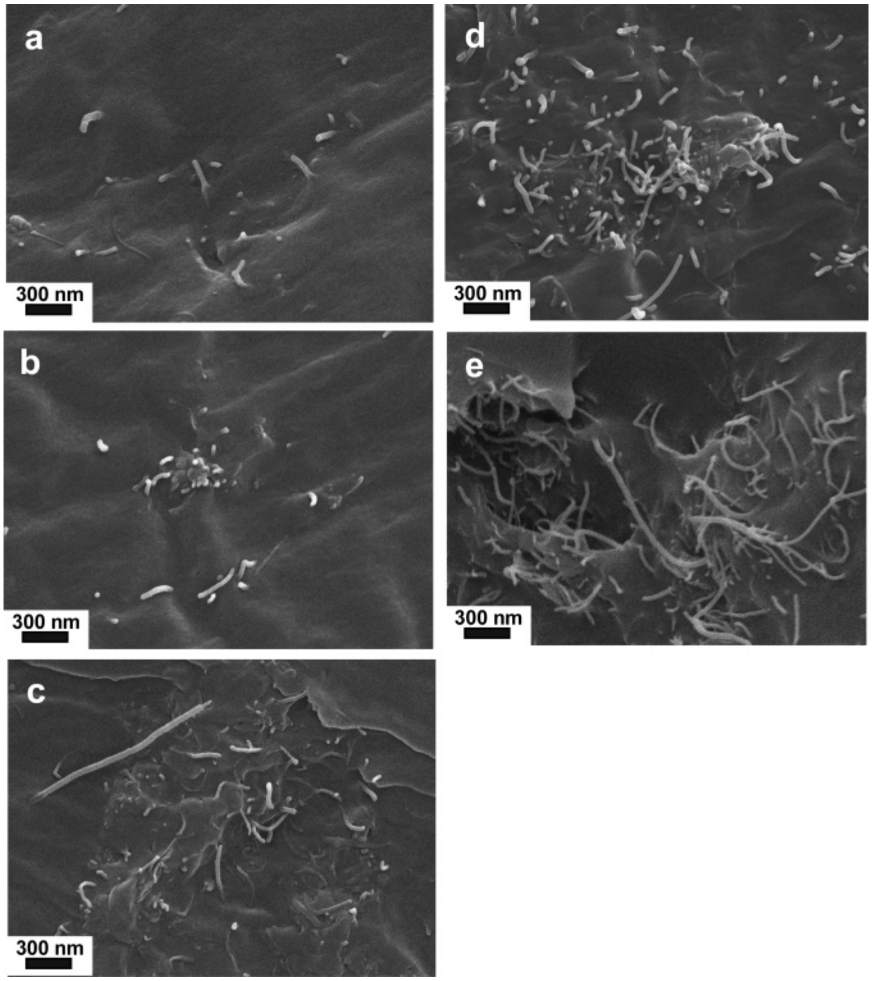

Figure 4. SEM images of fractured surface of the u-CNTs/epoxy nanocomposite loaded with different CNT contents: (a) 0.1 wt %, (b) 0.3 wt %, (c) 0.5 wt %, (d) 0.7 wt %, and (e) 1.0 wt %.

neity and dispersion on the fracture surface. A number of bundles is found to have broken rather than just having pulled out of the surface, demonstrating that strong interfacial bonding exists between the epoxy matrix and the functionalized nanotubes. As the loading of the CNTs-MA increases, good dispersion is still achieved, and most of the CNTs-MA are embedded and tightly held to the matrix (Figure 5a−e). The same results can be obviously observed in TEM images of a cross-section of the CNT/epoxy nanocomposites (see the Supporting Information).

Tensile Properties of the CNTs/Epoxy Nanocomposites. Figure 6 shows the effect of the CNT content on the mechanical properties, including tensile strength (Figure 6a), elongation-at-break (Figure 6b), and tensile modulus (Figure 6c), according to all of the CNTs/epoxy nanocomposites. For the CNTs-MA system, the tensile strength increases with the CNTs-MA content: the presence of the strong chemical bonding formed by the reaction between the CNTs-MA and the epoxy molecules results in good compatibility between these two phases. The average tensile strength is 50% higher than pristine EPOn 828 epoxy with the addition of 1.0 wt % CNTs-MA. For the u-CNT/epoxy nanocomposites of 0.1 wt %, the tensile strength only slightly increases. As the loading of the u-CNTs goes beyond 0.1 wt %, the system shows a decrease in tensile strength due to defects that are caused by the aggregation of the u-CNTs in the epoxy matrix.

Conceptually, inorganic/organic composites are often expected to become stiff and more brittle upon incorporation of inorganic fillers. However, carbon nanotubes present a particular form of reinforcing fiber, with a high aspect ratio and highly flexible elastic behavior during loading, which are very different from micrometer-sized fibers. Attractively, through the introduction of the CNTs-MA into the epoxy matrix, because of strong chemical bonds, the elasticity of the nanocomposites is affected, increasing the strain-at-break along with the CNTs-MA content until 0.7 wt %. The plasma-modified nanotubes exhibited an increase of ultimate elongation up to 43%, which is a 380% increase as compared to the relatively brittle pristine epoxy matrix. The improvement in elasticity in the case of the compatible CNTs-MA/epoxy nanocomposites can be attributed to the load transfer from the epoxy matrix to CNTs-MA reinforcement via strong chemical bonding, thereby increasing elongation in the epoxy polymer. As the loading of the CNTs-MA increases to 1.0 wt %, the result for elongation-at-break is lower than that of the 0.7 wt % but is still higher than the pristine epoxy resin. The reason may result from the existence of the defects arising from the aggregation of high amounts of the CNTs-MA addition. For the u-CNTs system, the elongation-at-break increases at the low CNT content of 0.1 wt % and starts to decrease as the addition of u-CNTs is more than 0.1 wt %,

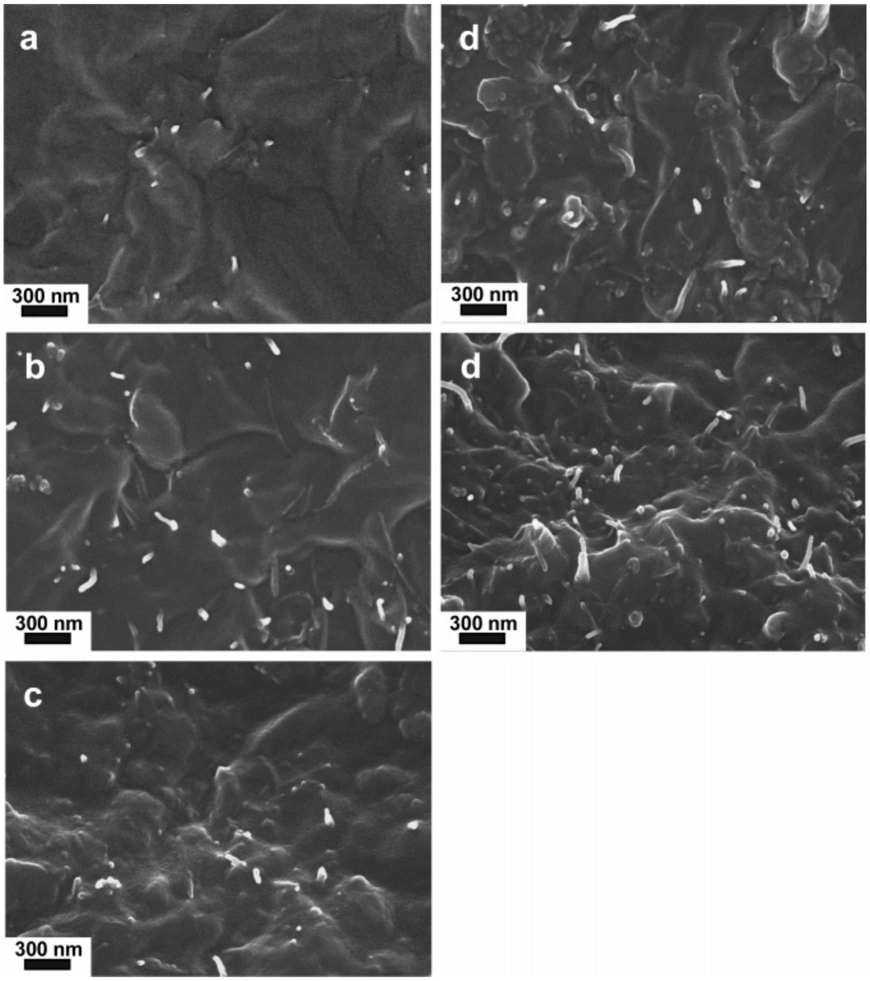

Figure 5. SEM images of fractured surface of the CNTs-MA/epoxy nanocomposites loaded with different CNT contents: (a) 0.1 wt %, (b) 0.3 wt %, (c) 0.5 wt %, (d) 0.7 wt %, and (e) 1.0 wt %.

due to the lack of a strong affinity between the u-CNTs and the epoxy matrix.

The tensile modulus in these two systems increases with the loading of the CNTs (Figure 6c); however, the CNTs-MA system is superior to the u-CNT system in terms of tensile modulus. The tensile modulus shows more than 100% improvement at just 1.0 wt % loading of the CNTs-MA, as compared to a 42% increase for the u-CNTs. The result shows that the tensile modulus obtained using the CNTs-MA is higher than that of the u-CNTs and can be attributed to the fact that the functionalized nanotubes have better dispersion inside the epoxy matrix, leading to greater surface areas, which in turn provide more interactions between the CNTs-MA and the epoxy matrix. Moreover, the CNTs-MA with amino groups attached are expected to form a highly cross-linked structure, increasing the stiffness of the epoxy matrix as the CNTs-MA content increases. In summary, higher tensile moduli are obtained in the chemically bonded and compatible CNTs-MA/epoxy nanocomposites.

Thermal Properties of the CNTs/Epoxy Nanocomposites. Figure 7a presents the effect of CNT content on the thermal decomposition temperature (T_d) at 5 wt % weight loss, revealing that the addition of the CNTs increases T_d for the CNTs/epoxy nanocomposites. Additionally, the enhancement of the thermal stability of the CNTs-MA system is more marked than that of the u-CNTs system. The CNTs-MA, which have strong chemical bonding and are more compatible with the epoxy matrix, can be inferred to act as gas barriers that prevent the permeation of volatile gas out of the nanocomposites during thermal decomposition. Furthermore, the strong bonding interactions between CNTs-MA and epoxy matrix lead to the restriction of the thermal motion of the epoxy molecules, causing these CNTs-MA/epoxy nanocomposites to have a better thermal stability than the pristine epoxy resin. By contrast, the u-CNTs system shows a slight increase in the decomposition temperature (from 368 to 378 °C), as compared with the CNTs-MA system (from 368 to 389 °C), due to the existence of only weak interactions and poor dispersion inside the epoxy matrix. As a result, the small increase of the decomposition temperature in the u-CNTs system may derive from the incorporation of the inorganic u-CNTs inside the epoxy matrix.

Figure 7b shows the effect of CNT content on T_g for all of the CNT/epoxy nanocomposites. The T_g increases with the CNT content for both of the CNT/epoxy nanocomposites. However, the increase in the value of T_g in the CNTs-MA system is greater than that in the u-CNTs system. The functionalized nanotubes have strong interactions between the CNTs-MA and the epoxy matrix; via the amino groups that provide the chemical bonding between these two phases, reducing the mobility of main chains of the epoxy molecules.

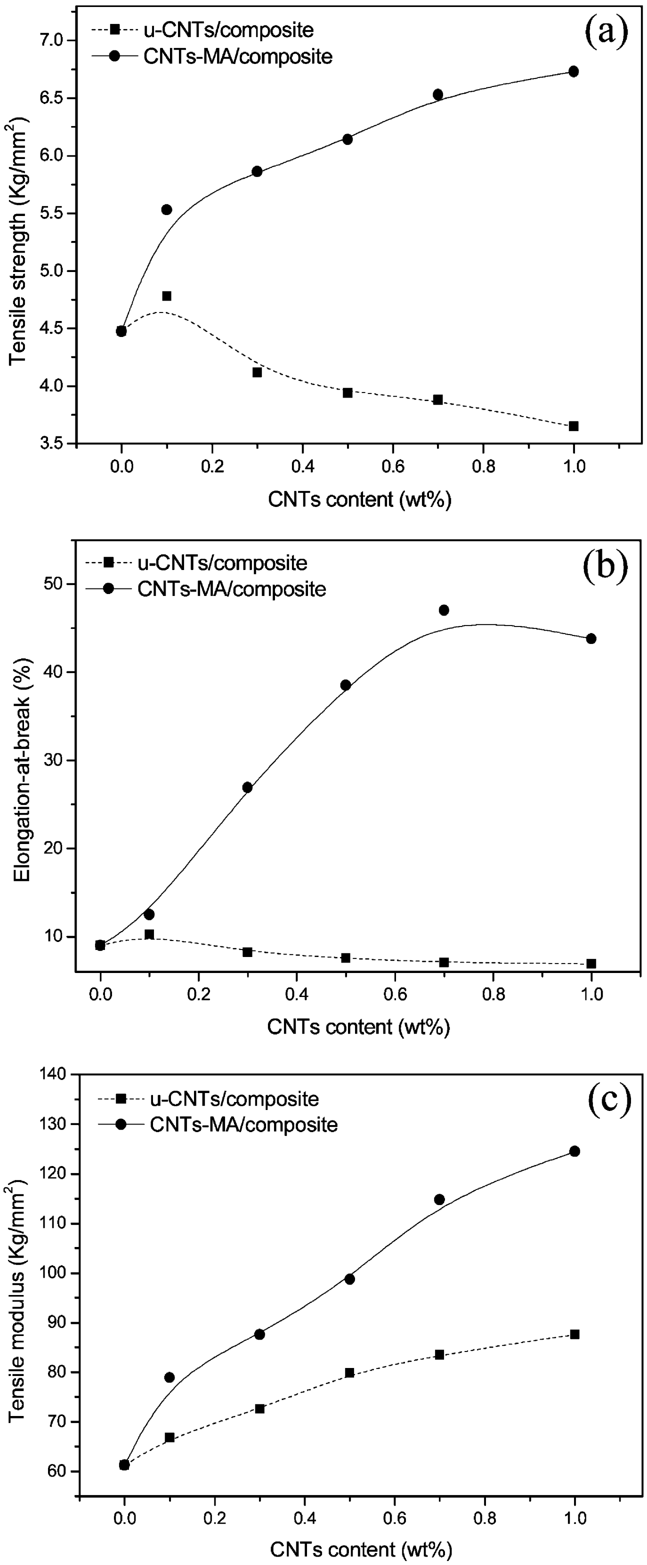

Figure 6. Effect of the CNT content on the (a) tensile strengths, (b) elongation-at-breaks, and (c) tensile moduli of the CNTs/epoxy nanocomposites.

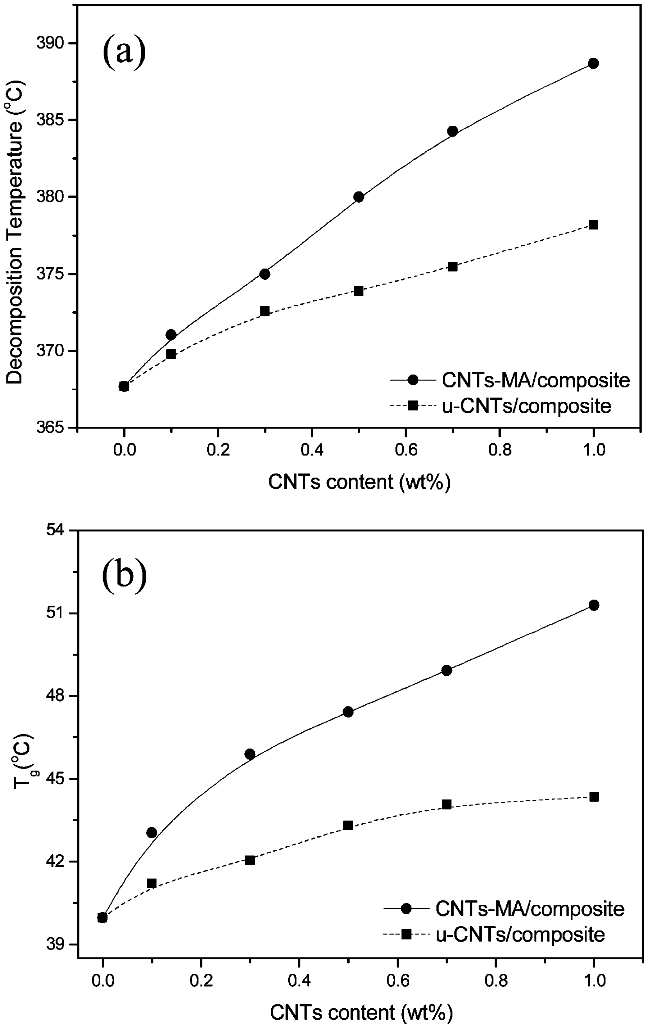

Figure 7. Effect of CNT content on the (a) T_d at 5 wt % weight loss and (b) T_g. The upper curve is the CNTs-MA/epoxy nanocomposite, and the lower curve is the u-CNTs/epoxy nanocomposite.

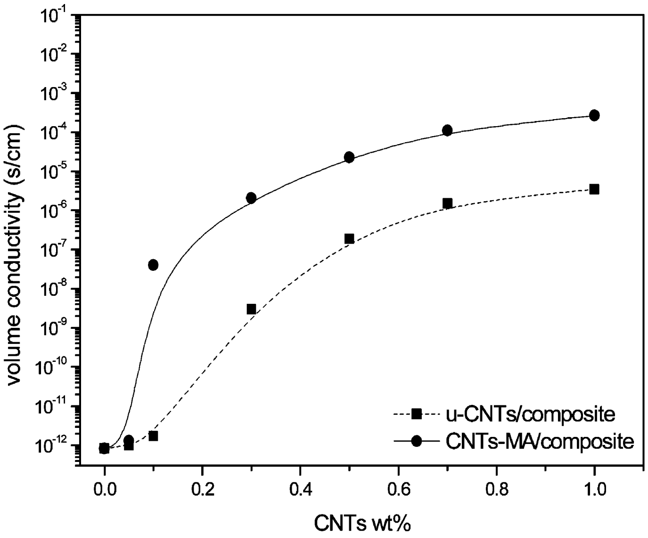

Figure 8. Comparative plot of the AC conductivity of the CNTs/epoxy nanocomposite as a function of the CNT content.

Hence, the T_g of the CNTs-MA/epoxy system increases much more markedly as compared with the u-CNTs/epoxy system. In summary, the plasma-modified CNTs-MA system is more thermally stable than the u-CNT system or the pristine epoxy resin.

Electrical Properties of the CNTs/Epoxy Nanocomposites. Figure 8 is the comparative plot of the AC conductivity of the CNTs/epoxy nanocomposites as a function of the CNT content. It shows that conductivity increases with CNT content for both types of system. However, the CNTs-MA/epoxy system shows a lower percolation threshold (around

0.1 to ~0.2 wt %) than the u-CNTs/epoxy system (around 0.5 to ~0.6 wt %). The reason may be explained as follows: the well-dispersed CNTs-MA inside the epoxy matrix can easily contact each other and therefore reduce the amount of CNTs needed to construct a conductive pathway. Moreover, with the increase of CNT loading, the CNTs-MA/epoxy system can achieve a conductivity of 2.6×10^{-4} S/m with 1.0 wt % addiction, which is 2 orders higher than the u-CNTs/epoxy systems (3.5×10^{-6} S/m).

A crucial parameter for the production of the conductive epoxy nanocomposites is the control of the degree of the grafting on the tube walls. The degree of grafting should not be too high, to avoid significantly disturbing the π-electron system of the tube walls, or even insulating the CNTs from the epoxy matrix. However, it should be sufficient to provide good compatibility between the CNTs and the epoxy matrix.[14] In this study, from XPS results, the percentage of the maleic anhydride grafted onto the tube walls is 6.4 wt %, which was controlled according to our designated value to obtain superior mechanical and electrical epoxy nanocomposites. The advantage of the plasma-induced grafting polymerization is that not only the degree of grafting on the CNTs can be controlled by altering plasma-treatment conditions but also that this method can be extended to other polymer systems to obtain various CNT/polymer nanocomposites.

Conclusion

The MA molecule was successfully grafted onto the MWNTs via a plasma-induced method, forming functionalized nanotubes, CNTs-MA. The functionalized nanotubes can be incorporated into the epoxy composites through the formation of strong covalent bonding in the course of epoxy curing reactions and, as a result, become an integral structural component of the cross-linked epoxy system. The results obtained show that the CNTs-MA/epoxy nanocomposites had a good dispersion of nanotubes inside the epoxy matrix, as well as an improvement in mechanical properties. Moreover, the CNTs-MA/epoxy nanocomposites not only demonstrated superior mechanical properties but also functioned as conductive nanocomposites for the purpose of electrostatic discharge and electromagnetic−radio interference protection materials. Therefore, the method for developing fully integrated nanotube−epoxy composites by plasma-induced grafting polymerization can be extended to other polymer systems and provide a variety of hybrid materials.

Acknowledgment. The authors thank the National Science Council of the Republic of China for financially supporting this research under Contract NSC93-2218-E-006-002 and the Taiwan Textile Research Institute.

Supporting Information Available: Three additional figures including IR spectrum and TEM images. This material is available free of charge via the Internet at http://pubs.acs.org.

CM062277P